Photoluminescence spectrum and dynamics in oxidized silicon nanocrystals: A nanoscopic disorder system

Yoshihiko Kanemitsu
Institute of Physics, University of Tsukuba, Tsukuba, Ibaraki 305, Japan
(Received 24 July 1995)

We have studied luminescence properties of nanometer-sized Si crystallites fabricated by laser breakdown of SiH_4 gas. An exponential absorption tail is observed and red photoluminescence (PL) appears in the exponential tail. The PL decay behavior is characterized by a stretched exponential function. At higher temperatures, the effective PL decay rate τ^{-1} depends exponentially on the monitored phonon energy $\hbar\omega$: $\tau^{-1} \propto \exp(\hbar\omega/E_\tau)$, where E_τ is a constant depending on temperature. On the other hand, at low temperatures, the PL lifetime is almost independent of the PL wavelength and phonon-related structures in the PL spectrum are not clearly observed under resonance excitation. The order and disorder natures of Si nanocrystallites are discussed. [S0163-1829(96)03619-3]

I. INTRODUCTION

The discovery of efficient visible luminescence in Si,[1] Ge,[2] and SiC (Ref. 3) nanocrystallites has stimulated considerable efforts in understanding optical properties of group-IV semiconductor nanocrystallites and producing different nanocrystallite devices. In particular, porous silicon[4,5] and Si nanocrystallites are receiving widespread interest motivated by potential applications as light-emitting devices compatible with silicon-based optoelectronic integrated circuits. There are many extensive studies concerning the origin of visible light emission, the improvement of luminescence efficiency, and the tuning of luminescence wavelength. However, the mechanism of visible luminescence is not clear and is currently under discussion[6–10] because porous silicon and Si nanocrystallites show various optical characteristics.

A drastic size reduction to a few nanometers is required for the observation of efficient visible light emission. With large surface-to-volume ratios in Si nanocrystallites, surface effects become more enhanced on decreasing the size of nanometer-sized crystallites. The photoluminescence (PL) peak wavelength and intensity are sensitive to the surface chemistry of porous silicon, particularly with regard to the amounts of oxygen and hydrogen on the surface. It is considered that surface effects as well as quantum confinement effects in porous silicon and Si nanocrystallites influence and complicate the mechanism of the visible luminescence.[7] For example, porous silicon and Si nanocrystallites show very broad PL and nonexponential PL decay in the time region from picoseconds to milliseconds.[5] Moreover, the electroluminescence[11] and PL (Ref. 12) wavelengths are sensitive to the excitation conditions such as applied voltage, laser pulse width, and laser intensity.

In this work we report luminescence properties of Si nanocrystallites capped by a SiO_2 thin layer. In order to understand unique and complicated luminescence properties of Si nanocrystallites, we need to study the optical properties of isolated Si nanocrystallites with an identical surface structure. The temperature dependence of the luminescence spectrum and dynamics is explained in terms of carrier localization in a disordered potential of surface states. The order and disorder natures of oxidized Si nanocrystallites are discussed.

II. EXPERIMENT

The nanometer-sized Si crystallites were produced by laser breakdown of SiH_4 gas. Details of the preparation and characterization of these nanocrystallite samples are given in Ref. 13. Here we briefly describe the sample preparation procedure. Pure SiH_4 gas was introduced into a vacuum chamber (a background pressure of $<10^{-6}$ Torr) and the pressure of SiH_4 gas was held at $\sim$10 Torr. Laser pulses ($\sim$200 mJ per pulse at 1.06 μm, 10-ns pulse duration) from a Nd^{3+}:YAG (yttrium aluminum garnet) laser system were focused. The Si nanocrystallites deposited on quartz substrates were oxidized at room temperature. Transmission electron microscopy, Fourier-transform infrared spectroscopy, and x-ray photoemission spectroscopy examinations indicated that the oxidized Si nanocrystallites consist of a c-Si sphere of the 3.7-nm average diameter and a 1.6-nm-thick amorphous SiO_2 (a-SiO_2) surface layer. For comparison, we have also prepared 40-μm-thick free-standing porous silicon films from p-type, 3.5-Ω cm Si wafers. Details of the preparation of porous silicon are given in Ref. 7.

The photoluminescence spectra were obtained by using Cd-He, He-Ne, Kr, and dye lasers. The measurement temperature was varied from 2 to 300 K in a cryostat. The time-resolved PL spectra of oxidized Si nanocrystallites were measured under 5-ns, 355-nm excitation (10-Hz repetition rate) using a boxcar signal averager. The spectral sensitivity of the measuring system was calibrated by using a tungsten standard lamp.

III. RESULTS AND DISCUSSION

Figure 1 shows optical absorption spectra in oxidized Si nanocrystallites, porous silicon, bulk crystalline Si (c-Si),[14] and hydrogenated amorphous Si (a-Si:H).[15] An exponential absorption tail (the Urbach tail) in Si nanocrystallites is observed in the near-infrared and visible regions. The absorp-

 © 1996 The American Physical Society

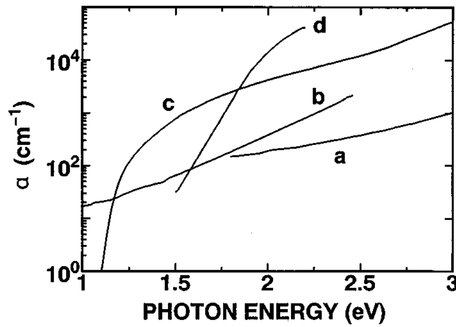

FIG. 1. Optical absorption spectra of (a) an oxidized Si crystallite sample with the average c-Si core diameter of 3.7 nm (αd spectrum), (b) porous silicon, (c) indirect-gap crystalline bulk Si (Ref. 14), and (d) amorphous Si:H (Ref. 15). Si nanocrystallites and porous silicon show exponential absorption spectra in the near-infrared and visible spectral regions.

tion spectrum is approximately given by

$$\alpha \propto \exp(\hbar\omega/E_{\alpha}), \tag{1}$$

where $\hbar\omega$ is the incident photon energy and E_{α} is the Urbach energy determining the exponential slope. In direct-gap semiconductor nanocrystallites, the peak of the lowest absorption band is clearly observed even in samples having broad crystallite size distributions.[16] However, featureless absorption spectra are observed in porous silicon and Si nanocrystallites. In Si nanocrystallites, the conduction band has a large density of size-quantized states. Phonon-assisted optical transitions near the lowest level cause the overlapping of optical transitions.[17,18] Then, it is speculated that one origin of featureless absorption spectra is the indirect-gap nature of Si nanocrystallites in the absorption process.

The absorption spectrum of the nanocrystallite sample is entirely different from that of indirect-gap bulk crystalline Si (c-Si). The exponential absorption tail (the Urbach energy $E_{\alpha}\sim$250 meV in Si nanocrystallites) is much larger than a-Si:H ($E_{\alpha}\sim$40–50 meV). Porous silicon and Si nanocrystallites are an interesting class of materials whose properties differ from those of single crystalline Si and amorphous Si. The large Urbach tail reflects the nanoscopic disorder nature of Si nanocrystallites, such as a distribution of crystallite size and shape and variations in surface roughness and surface structures. Therefore, it is considered that the featureless and exponential absorption spectrum reflects both the indirect-gap semiconductor nature of nanocrystallites and the nanoscopic disorder of nanocrystallites. This large Urbach energy causes the complicated PL behaviors in Si nanocrystallites, as will be shown below.

Red luminescence in our oxidized Si nanocrystallites is excited most efficiently by laser energies above 2.5 eV. Under 325-nm excitation at room temperature, a PL peak is around ~1.65 eV and the PL spectrum is very broad (~0.3 eV full width at half maximum) with a slightly asymmetric Gaussian shape. Efficient red luminescence appears within the exponential absorption tail. The PL peak energy is not sensitive to the crystallite size.[13] Only a very small blueshift of the PL peak energy appears with a decrease of crystallite size: The blueshift of the PL peak energy is 0.1 eV or less in a range between 3.5 and 13 mm. This size dependence of the

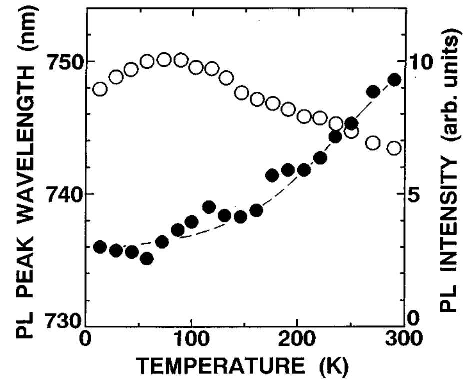

FIG. 2. Temperature dependence of the peak wavelength of the photoluminescence spectrum (solid circles) and the luminescence intensity (open circles) under weak cw 325-nm laser excitation. The broken line is a guide to the eye. At low temperatures below ~100 K, the luminescence peak energy is almost independent of temperature and the luminescence intensity decreases. The temperature dependence of the luminescence spectrum below ~100 K is different from that above ~100 K.

PL peak energy cannot be explained by the proposed ''pure'' quantum confinement theories.[19–21] Rather, the PL intensity is very sensitive to crystallite size and the surface oxidation condition. The broad PL is caused by light-emitting sites with broad energy distribution in Si nanocrystallites. The oxidized Si nanocrystallite sample is a disorder system as a set of nanometer-size crystalline spheres.

Figure 2 shows the temperature dependence of the PL peak wavelength and the PL intensity under 0.2-mW/cm^2, 325-nm excitation from a cw He-Cd laser. With a decrease of temperature, the PL peak wavelength becomes shorter. At low temperatures below about 100 K, the PL peak wavelength is not sensitive to temperature. Moreover, the PL intensity gradually increases with decreasing temperature until about 100 K and then decreases at low temperatures below 100 K. These temperature dependences of the PL peak wavelength and intensity imply that the microscopic processes determining PL properties at low temperatures are different from those at high temperatures. For a deeper understanding of this temperature dependence, we measured the temperature and wavelength dependence of the PL decay dynamics.

The PL decay profiles are nonexponential at the temperature between 10 and 300 K and they are well described by a stretched exponential function[22,23]

$$I(t)=I_0(\tau/t)^{1-\beta}\exp[-(t/\tau)^{\beta}], \tag{2}$$

where τ is an effective decay time, β is a constant between 0 and 1, and I_0 is a constant. The solid line in the inset of Fig. 3 is given by the above function. The least-squares fitting of the data gives the value of τ. This stretched exponential decay is usually observed in the PL decay and transport properties of disordered system.[22] The temperature and photon-energy dependences of the PL decay rate τ^{-1} are summarized in Fig. 3. At high temperatures, the PL decay time τ depends strongly on both the monitored PL photon energy and temperature. An exponential energy dependence of the PL decay rate τ^{-1} decay rate is observed: The decay rate is approximately given by

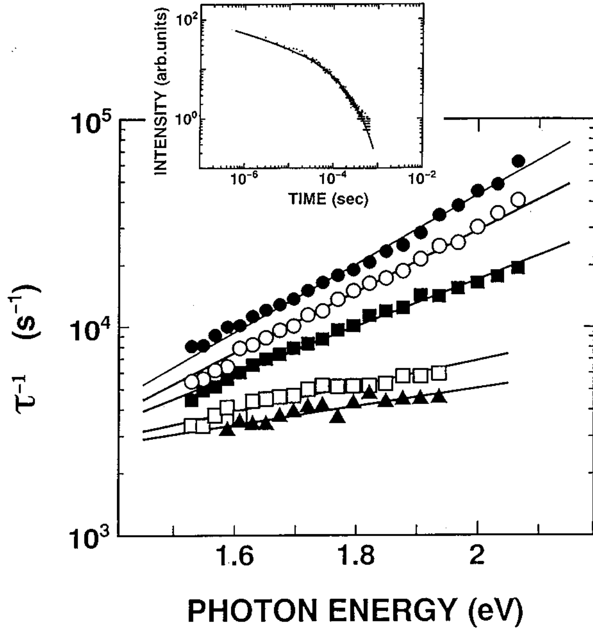

FIG. 3. Effective luminescence decay rate τ^{-1} as a function of the monitored photon energy at 280, 220, 150, 80, and 30 K. The exponential slope increases with increasing temperature. The inset is the double logarithmic plot of photoluminescence decay curve at 80 K and 1.65 eV. The solid line is a theoretical curve given by a stretched exponential function.

$$\tau^{-1} \propto \exp(\hbar\omega_{\mathrm{PL}}/E_0), \tag{3}$$

where E_0 is a constant depending on temperature and $\hbar\omega_{\mathrm{PL}}$ is the PL photon energy. On the other hand, at low temperatures below about 100 K, the PL decay rate is not sensitive to the PL phonon energy. The dominant physical process controlling PL properties at high temperatures is different from that at low temperatures.

If the decay of excited electrons and holes in nanocrystallites is determined by competing radiative τ_R and nonradiative τ_{NR}, the PL lifetime τ_{PL} and the PL quantum yield η are given by

$$\tau_{\mathrm{PL}}^{-1} = \tau_R^{-1} + \tau_{\mathrm{NR}}^{-1} \tag{4}$$

and

$$\eta = \tau_R^{-1}/(\tau_R^{-1} + \tau_{\mathrm{NR}}^{-1}). \tag{5}$$

The ratio η/τ_{PL} gives the temperature dependence of the radiative decay rate. The radiative decay rate depends strongly on the temperature, as shown in Fig. 4, where the relative PL intensity I is used instead of η. With decreasing temperature, the estimated radiative decay rate $R_r(=I/\tau_{\mathrm{PL}})$ increases. The temperature dependence of the radiative decay rate is given by

$$R_r \propto \exp(-E_r/kT), \tag{6}$$

where E_r is the thermal activation energy of the radiative decay rate. The solid line in Fig. 4 gives $E_r \sim 71$ meV. The temperature-dependent radiative lifetime means that the PL does not come from one state in the single crystallite. We need to consider the multilevel light-emitting states in the single crystallite.

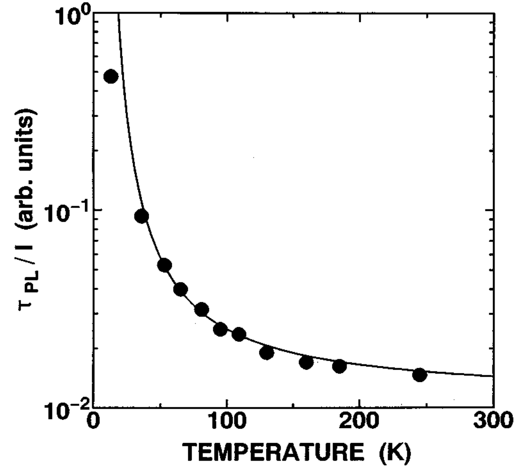

FIG. 4. Temperature dependence of the estimated radiative lifetime (the ratio of the luminescence lifetime to the luminescence intensity τ_{PL}/I). The solid line is a calculated one.

If the higher and lower states have the fast and slow decay rates, respectively, and there is the Boltzmann distribution between these states, the radiative decay rate is temperature dependent. A simple model is a two-level one consisting of the singlet and triplet exciton states in molecularlike materials. The activation energy E_r reported in porous silicon is 3–17 meV.[24,25] It is proposed that in porous silicon the thermal activation energy corresponds to the singlet-triplet splitting energy of the exciton states ($\Delta \sim 3-10$ meV).[6,25] The values of E_r and Δ in porous silicon are very small compared to $E_r \sim 71$ meV in our oxidized Si nanocrystallites. In particular, E_r in oxidized Si nanocrystallites is very large compared to the singlet-triplet splitting energy in nanocrystallites in porous silicon. Rather, the activation energy of 71 meV is close to the maximum of the phonon density of states in bulk c-Si of 61 meV. Therefore, for the activation process in the radiative decay rate in oxidized Si nanocrystallites, we consider phonon-limited processes rather than the singlet-triplet splitting mechanism.

The temperature dependence of the radiative lifetime is well described by the above relation of Eq. (6) at high temperatures. At low temperatures the radiative lifetime becomes very long. The PL properties at low temperatures will be affected by the very long relaxation processes. In fact, the temperature dependence of the PL properties at low temperatures is different from that at high temperatures (see Figs. 2 and 3). For the nonradiative recombination process, we consider tunneling[26] and thermally activated transport processes[25] of carriers to nonradiative recombination centers. Both tunneling and thermally activated nonradiative recombination rates depend on the barrier height E_a, where E_a is the barrier height measured from the lowest-energy level of the confined carrier. If a carrier has higher energy, the effective barrier height of this carrier becomes small. The nonradiative recombination rate of carriers in higher energy states is larger. Suemoto, Tanaka, and Nakajima[25] estimated that the barrier height for nonradiative recombination processes E_a is ~ 0.2 eV for the PL lifetime between microseconds and

milliseconds in porous silicon. The similar PL lifetime is observed in our Si nanocrystallites and the barrier E_a is also estimated to be 0.2–0.3 eV. This value is one order of magnitude lower than the band offset between Si and SiO_2. The Si nanocrystallites are isolated from each other in our samples. Then, it is considered that the carrier escape from a crystallite to another crystallite does not occur. The small barrier height (several hundred meV) implies that the carrier is localized in a disordered potential of surface states on c-Si spheres.

Let us consider the temperature dependence of the PL peak energy and the PL decay dynamics. The PL peak wavelength is not sensitive to the crystallite size. The size dependence of the PL peak wavelength in oxidized Si nanocrystallites is not explained by the proposed quantum confinement models,[19–21,27] as mentioned above. Here we assume that localized tail states in Si nanocrystallites play an essential role in radiative and nonradiative recombination processes. The shallow tail state is formed by the disordered potential of the surface states and this is due to the surface roughness and variations in surface stoichiometry. The exponential tail below the band edge is formed with small state density. The temperature dependence of the PL spectrum and dynamics suggests that the PL decay properties at high temperatures are controlled by thermally activated process. The cascade of carriers from higher states to lower states makes the lifetime of higher states shorter and then the exponential slope is observed. This thermal cascade process causes the PL peak wavelength to shift to the long wavelength with increasing temperature, as shown in Fig. 2. At low temperatures, the PL decay rate is not sensitive to the PL energy and the PL peak energy is not sensitive to temperature. The temperature-insensitive PL properties suggest that the thermally activated process is negligible at low temperatures. Because the radiative lifetime is very long at temperature below 100 K, the slow tunneling process affects the PL properties.[25,26] The long PL lifetime ($\tau_{PL}>0.3$ ms at $T<100$ K) is mainly determined by the tunneling process and then PL peak energy is almost independent of temperature. The thermally activated or tunneling processes of carriers in tail states determine PL properties of oxidized Si nanocrystallites.

The transient PL spectrum is sensitive to the laser excitation intensity. With an increase of excitation intensity of 5-ns, 355-nm laser pulses, a blueshift of the PL peak energy is observed, as shown in Fig. 5. These large shifts are not observed in bulk c-Si and a-Si:H. Since Si nanocrystallites show large Urbach energy and long PL lifetime, the state filling easily occurs in the lower-energy states under high excitation conditions. Then, we can observe the blueshift of the PL peak energy at the initial stage. A rapid redshift of the PL wavelength is also observed with delay time. This redshift shows that the recombination rate becomes larger at higher-energy states, and is caused by the cascade of carriers from higher states to lower states. The excitation-power-sensitive PL spectrum suggests that shallow tail states with small state density exist in Si nanocrystallites. Our experimental results can be more easily understood in terms of the localization of carriers or excitons in a disorder potential of surface states on c-Si spheres.

The oxidized Si nanocrystallite sample shows the broad PL spectra similar to porous silicon under laser excitation at

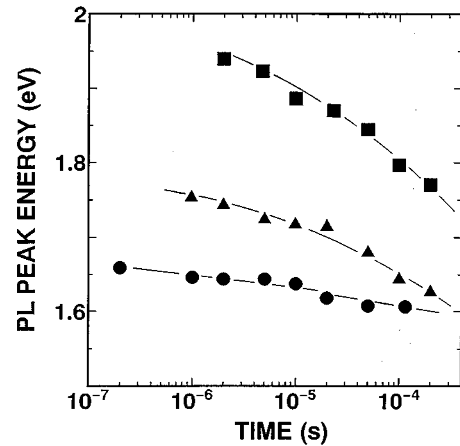

FIG. 5. Luminescence peak energy versus delay time under a 5-ns, 355-nm laser excitation of 0.64, 10.5, and 113 μJ/cm^2. With an increase of the excitation laser intensity, the blueshift of the luminescence peak energy occurs at the initial stage and the redshift of the luminescence peak energy with time delay is clearly observed.

energies above ~2.2 eV. However, by reducing the excitation energy below 2 eV, steplike phonon structures due to coupling TO phonons and TA phonons are clearly observed in porous silicon at low temperatures.[6,28,29] In Fig. 6 we show the PL spectrum of porous silicon under 1.959-eV excitation at 2 K. Energy positions of the singlet-triplet splitting energy of the excitons states ($\Delta=5$ meV),[6] TO phonons (57.3 meV), and TA phonons (18.2 meV) are indicated. Phonon-related steplike structures are clearly observed in porous silicon under resonance excitation. These steplike structures are different from those of a-Si:H (Ref. 30) and porous a-Si:H (Ref. 29) under resonant excitation. However, under the same experimental condition, clear phonon-related structures are not observed in oxidized Si nanocrystallites, although a very weak step seems to be near 60 meV. Phonon-related structures in porous silicon are much sharper than those in oxidized Si nanocrystallites at least. In porous silicon, the step-

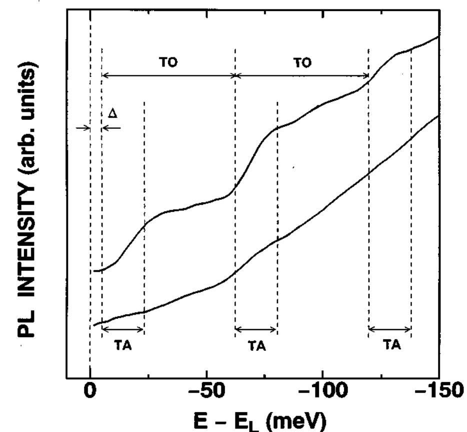

FIG. 6. Luminescence spectra in porous silicon (upper part) and oxidized Si nanocrystallite (lower part) samples under 1.959-eV excitation at 2 K. Phonon-related structures in the luminescence spectrum are clearly observed in porous silicon under resonant excitation at low temperatures.

like phonon structures are mainly caused by the sample inhomogeneity of porous silicon,[6] but the peak structure is expected in idealized nanoparticles. The steplike structure in the PL spectrum depends on the measurement temperature, the sample preparation condition, and the laser excitation condition.[29] The quantitative explanation of the steplike spectrum is still in dispute.

While luminescence data of oxidized Si nanocrystallites and porous silicon are similar in many ways (e.g., the broad PL spectrum in the red spectral region, nonexponential PL decay in the microsecond to millisecond time region, and the size-insensitive PL spectrum), there are some important differences as mentioned above (the activation energy for radiative recombination and the phonon-related structure in the PL spectrum). Luminescence properties depend on the nanoscopic inhomogeneity of the samples, such as the surface structures of nanocrystallites and the size distribution of nanocrystallites. The large activation energy for the radiative recombination and indistinct phonon-related structures in the PL spectrum show that a potential fluctuation in surface states in oxidized Si nanocrystallites is much larger than that in porous silicon. The disordered potential of oxidized surface states causes the shallow tail or localized states. The broad PL spectrum and nonexponential PL decay imply the existence of shallow tail states below the band edge in oxidized Si nanocrystallites. It is considered that the broad energy distribution of the radiative and nonradiative recombination centers in the *single* crystallite mainly determines the luminescence properties in isolated Si nanocrystallites. Oxygen-modified surface states play active roles in luminescence processes.

In porous silicon, the shape of nanocrystallites is not spherical and the surface structure of nanocrystallite is terminated by silicon hydrides, silicon oxyhydrides, and silicon oxides. Nanocrystallites with different surface structures exist in porous silicon. After air exposure or surface oxidation, porous silicon shows stable and efficient red luminescence.[6,31] Oxygen-modified surface states play an essential role in efficient luminescence processes even in porous silicon. On the other hand, it is considered that phonon-related structures in PL spectra under resonance excitation are more sensitive to the disorder of crystallite surface. The ordering of nanocrystallites depends on the bonding of the surface atoms. Raman spectroscopy examinations imply that hydrogen-terminated porous silicon shows the crystalline nature while oxygen-terminated porous silicon shows atomic disorder within the nanoparticles.[32] Hydrogen termination extremely reduces the surface recombination centers in bulk *c*-Si.[33] The role of hydrogen-terminated nanocrystallites in luminescence in porous silicon is not clear. The microscopic understanding of surface states in Si nanocrystallites reveals the details of visible luminescence mechanism and the origin of steplike structures at low temperatures. For a deeper understanding of electronic and optical properties of Si nanocrystallites, we should try to prepare fully hydrogen-terminated Si nanocrystallites and discuss their optical properties.

IV. CONCLUSION

In conclusion, we have studied dynamics and spectroscopy of isolated oxidized Si nanocrystallites. The crystalline Si spheres with a disorder potential of surface states show complicated luminescence properties. Oxygen-modified surface states play an essential role in radiative recombination processes. We pointed out that while luminescence properties of oxidized Si nanocrystallites are similar to those of porous silicon in many ways, there are some differences: Phonon-related structures in the PL spectrum in porous silicon are much sharper than those of oxidized Si nanocrystallites under resonance excitation at low temperatures. Our experimental results in oxidized Si nanocrystallites are understood in terms of the localization of carriers or excitons in a disorder potential of surface states on *c*-Si spheres. The Si nanocrystallite sample is a nanoscopic disorder system in the sense that it has a distribution of the crystalline size and shape and a fluctuation of the surface structure and surface stoichiometry. The nanoscopic inhomogeneity will produce the unique optical properties of oxidized Si nanocrystallites and porous silicon.

ACKNOWLEDGMENTS

The author would like to thank H. Uto and S. Okamoto for the experimental assistance. This work was partly supported by a Grant-In-Aid for Scientific Research from the Ministry of Education, Science and Culture of Japan, the Konica Imaging Science Foundation, and the Iwatani Naoji Foundation.

[1] H. Takagi, H. Ogawa, Y. Yamazaki, A. Ishizaki, and T. Nakagiri, Appl. Phys. Lett. **56**, 2349 (1990).

[2] Y. Maeda, N. Tsukamoto, Y. Yazawa, Y. Kanemitsu, and Y. Masumoto, Appl. Phys. Lett. **59**, 3168 (1992).

[3] T. Matsumoto, J. Takahashi, T. Tamaki, T. Futagi, H. Mimura, and Y. Kanemitsu, Appl. Phys. Lett. **64**, 226 (1994).

[4] L. D. Lockwood, Solid State Commun. **92**, 101 (1994).

[5] Y. Kanemitsu, Phys. Rep. **263**, 1 (1995).

[6] P. D. J. Calcott, K. J. Nash, L. T. Canham, M. J. Kane, and D. Brumhead, J. Phys. Condens. Matter **5**, L91 (1993); J. Lumin. **57**, 257 (1993).

[7] Y. Kanemitsu, H. Uto, Y. Masumoto, T. Matsumoto, T. Futagi, and H. Mimura, Phys. Rev. B **48**, 2827 (1993).

[8] F. Koch, V. Petova-Koch, and T. Muschik, L. Lumin. **57**, 271 (1993).

[9] S. M. Prokes, W. E. Carlos, and O. J. Glembocki, Phys. Rev. B **50**, 17 093 (1994).

[10] E. Martin, C. Delerue, G. Allan, and M. Lannoo, Phys. Rev. B **50**, 18 258 (1994).

[11] A. Bsiesy, F. Muller, M. Ligeon, F. Gaspard, R. Herino, R. Romestain, and J. C. Vial, Phys. Rev. Lett. **71**, 637 (1993).

[12] Y. Kanemitsu and T. Matsumoto, in *Proceedings of the 22nd International Conference on the Physics of Semiconductors, Vancouver, 1994*, edited by D. J. Lockwood (World Scientific, Singapore, 1994), p. 2153.

[13] Y. Kanemitsu, T. Ogawa, K. Shiraishi, and K. Takeda, Phys. Rev. B **48**, 4883 (1993).

[14] W. C. Dash and R. Newman, Phys. Rev. **99**, 1151 (1955).

[15] R. A. Street, Philos. Mag. B **37**, 35 (1978).

[16] A. Nakamura, T. Tokizaki, H. Akiyama, and T. Kataoka, in *Optical Properties of Solids*, edited by K. C. Lee, P. M. Hui, and T. Kushida (World Scientific, Singapore, 1991), p. 284.

[17] L. E. Brus, P. F. Szajowski, W. L. Wilson, T. D. Harris, S. Schuppler, and P. H. Citrin, J. Am. Chem. Soc. **117**, 2915 (1995).

[18] M. S. Hybertsen, Phys. Rev. Lett. **72**, 1514 (1994).

[19] T. Takagahara and K. Takeda, Phys. Rev. B **46**, 15 578 (1992).

[20] J. P. Proot, C. Delerue, and G. Allan, Appl. Phys. Lett. **61**, 1948 (1992).

[21] L. W. Wang and A. Zunger, J. Chem. Phys. **100**, 2394 (1994).

[22] K. L. Ngai, Comments Solid State Phys. **9**, 127 (1979); **9**, 141 (1980).

[23] Y. Kanemitsu, Phys. Rev. B **48**, 12 357 (1993).

[24] G. W. 't Hooft, Y. A. R. R. Kessener, G. L. J. A. Rikken, and A. H. J. Venhuizen, Appl. Phys. Lett. **61**, 2344 (1992).

[25] T. Suemoto, K. Tanaka, and A. Nakajima, in *Light Emission from Novel Silicon Materials*, edited by Y. Kanemitsu, M. Kondo, and K. Takeda (The Physical Society of Japan, Tokyo, 1994), p. 190.

[26] J. C. Vial, A. Bsiesy, F. Gaspard, R. Herino, M. Ligeon, F. Muller, R. Romestain, and R. M. Macfarlane, Phys. Rev. B **45**, 14 171 (1993).

[27] S. Schuppler, S. L. Friedman, M. A. Marcus, D. L. Adler, Y. H. Xie, R. M. Ross, T. D. Harris, W. L. Brown, Y. J. Chabal, L. E. Brus, and P. H. Citrin, Phys. Rev. Lett. **72**, 2648 (1994).

[28] T. Suemoto, K. Tanaka, A. Nakajima, and T. Itakura, Phys. Rev. Lett. **70**, 3659 (1993).

[29] M. Rosenbauer, S. Finkbeiner, E. Bustarret, J. Weber, and M. Stutzmann, Phys. Rev. B **51**, 10 539 (1995).

[30] S. O. Gu, P. C. Taylor, and R. Ristein, J. Non-Cryst. Solids **137/138**, 591 (1991).

[31] V. M. Dubin, F. Ozanam, and J. N. Chazalviel, Phys. Rev. B **50**, 14 867 (1994); H. Mimura, T. Matsumoto, and Y. Kanemitsu, in *Microcrystalline and Nanocrystalline Semiconductors*, edited by R. W. Collins, C. C. Tsai, M. Hirose, F. Koch, and L. Brus, MRS Symposia Proceedings No. 358 (Materials Research Society, Pittsburgh, 1995), p. 635.

[32] J. C. Tsang, M. A. Tischler, and R. T. Collins, Appl. Phys. Lett. **60**, 2279 (1992).

[33] E. Yablonovitch, D. L. Alara, C. C. Chang, T. Gmitter, and T. B. Bright, Phys. Rev. Lett. **57**, 249 (1986).